

## Sparsity-driven distributed array imaging

Liu, D.; Kamilov, U.; Boufounos, P.T.

TR2015-140 December 13, 2015

### Abstract

We consider multi-static radar with a single transmitter and multiple, spatially distributed, linear sensor arrays, imaging an area with several targets. Assuming that the location and orientation of all the sensor arrays is known and that all measurements are synchronized, we develop compressive sensing based methods to improve imaging performance. Our approach imposes sparsity on the complex-valued reconstruction of the region of interest, with the non-zero coefficients corresponding to the imaged targets. Compared to conventional delay-and-sum approaches, which typically exhibit aliasing and ghosting artifacts due to the distributed small-aperture arrays, our sparsity-driven methods improve the imaging performance and provide high resolution. We validate our methods through numerical experiments on simulated data.

*IEEE International Workshop on Computational Advances in Multi-Sensor Adaptive Processing (CAMSAP) 2015*

© 2015 MERL. This work may not be copied or reproduced in whole or in part for any commercial purpose. Permission to copy in whole or in part without payment of fee is granted for nonprofit educational and research purposes provided that all such whole or partial copies include the following: a notice that such copying is by permission of Mitsubishi Electric Research Laboratories, Inc.; an acknowledgment of the authors and individual contributions to the work; and all applicable portions of the copyright notice. Copying, reproduction, or republishing for any other purpose shall require a license with payment of fee to Mitsubishi Electric Research Laboratories, Inc. All rights reserved.



# Sparsity-Driven Distributed Array Imaging

Dehong Liu, Ulugbek S. Kamilov, and Petros T. Boufounos  
Mitsubishi Electric Research Laboratories  
201 Broadway, Cambridge, MA 02139  
Email: {liudh, kamilov, petrosb}@merl.com

**Abstract**—We consider multi-static radar with a single transmitter and multiple, spatially distributed, linear sensor arrays, imaging an area with several targets. Assuming that the location and orientation of all the sensor arrays is known and that all measurements are synchronized, we develop compressive sensing based methods to improve imaging performance. Our approach imposes sparsity on the complex-valued reconstruction of the region of interest, with the non-zero coefficients corresponding to the imaged targets. Compared to conventional delay-and-sum approaches, which typically exhibit aliasing and ghosting artifacts due to the distributed small-aperture arrays, our sparsity-driven methods improve the imaging performance and provide high resolution. We validate our methods through numerical experiments on simulated data.

## I. INTRODUCTION

In order to image a scene, radar systems emit pulses and record echoes reflected from the targets in the scene. The received echoes are a weighted combination of the transmitted pulses, appropriately delayed according to the round-trip travel time from the transmitter to each target and back to each receiver, and scaled according to each target’s reflectivity. The radar reconstructs the scene from the received echoes by estimating the delay and reflectivity to each target. The angular (azimuth) resolution of radar images depends on the aperture size of the radar sensor while the distance (range) resolution depends on the bandwidth of the transmitted pulse.

In practice, it is often difficult or very expensive to build a large aperture to achieve high azimuth resolution. Instead, multiple distributed sensing platforms are often deployed, each with a small aperture size, collaboratively collecting radar echoes, thus creating a large effective aperture. Distributed sensing has several benefits, including flexibility of platform placement, low operation and maintenance cost, and robustness to individual sensor failures.

On the other hand, distributed sensing requires much more sophisticated processing, compared to a conventional single-array system. In practice, conventional distributed radar imaging approaches typically process the signals received at each sensor platform individually using matched filtering, then fuse these estimates in a subsequent stage. Since the platforms are not generally uniformly distributed, the final images may exhibit ambiguity or ghost images, making it difficult to distinguish targets.

In this paper, we aim to improve the imaging performance using distributed sensing by jointly processing all measurements and exploiting algorithms based on compressive sensing (CS). CS allows robust reconstruction of signals using a significantly smaller number of measurements compared to

their Nyquist rate. This sampling rate reduction is achieved by using randomized measurements, improved signal models, and non-linear reconstruction algorithms [1]. In radar applications, CS has been utilized to improve the resolution of images [2]–[5] by assuming that the received signal can be modeled as a linear combination of waveforms corresponding to the targets and the underlying vector of target reflectivity is sparse or has further structure.

Specifically, we consider a scenario where multiple small aperture arrays collect radar echoes from multiple targets excited by a single transmitter. The multiple arrays are uniform linear arrays randomly distributed with different locations and orientations at the same side of the area of interest. Although the image resolution of each array is low due to its small aperture size, a high resolution is achieved by combining all distributed arrays using sparsity-driven imaging method.

This paper is organized as follows. In Section II, we describe the model of distributed sensing, as well as the conventional delay-and-sum imaging approaches. We present our CS inspired imaging methods in Section III, where we propose algorithms based on spatial-domain and spatial-gradient-domain sparsity, respectively. Finally, we present numerical simulations followed by concluding remarks in Section IV.

## II. DISTRIBUTED SENSING MODEL

We consider a multi-static distributed radar with one transmitter and  $M$  distributed linear antenna arrays, each with  $N_m$  ( $m = 1, \dots, M$ ) elements, illuminating an area of interest. We assume the antennas arrays are static and placed at the same side of the area with random orientations within a certain angular range, as shown in Fig. 1.

We use  $p(t)$  to denote in the time-domain pulse emitted by the transmitter located at the spatial location  $\mathbf{l}_S$  represented by the red x-mark in Fig. 1. In the frequency domain, the pulse, denoted using  $P(\omega)$ , can be expressed as

$$P(\omega) = \int_{\mathbb{R}} p(t)e^{-j\omega t} dt. \quad (1)$$

For a single point target, located at location  $\mathbf{l}_T$ , the radar echo received by the  $n$ th element of the  $m$ th receiver array—the location of which is denoted using  $\mathbf{l}_{m,n}$ —can be expressed in the frequency domain as

$$Y(\omega, \mathbf{l}_S, \mathbf{l}_{m,n}) = P(\omega)X(\mathbf{l}_T)e^{-j\omega \frac{\|\mathbf{l}_S - \mathbf{l}_T\| + \|\mathbf{l}_{m,n} - \mathbf{l}_T\|}{c}}, \quad (2)$$

where  $X(\mathbf{l}_T)$  is the complex-valued reflectivity coefficient of the point target and the exponential term approximates the Green’s function from the source at  $\mathbf{l}_S$  to the receiver at

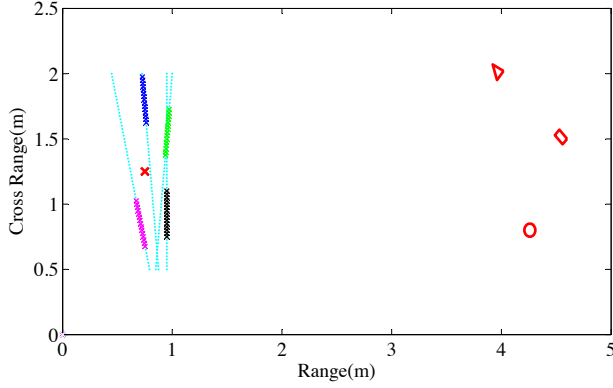


Fig. 1. Example distributed radar imaging configuration using distributed arrays, depicted using magenta, blue, green, and black color. The red x-mark represents transmitter and cyan dots represent virtual receivers from which missing data is reconstructed using one of the algorithms proposed in this paper. The red triangle, rectangle and circle on the right hand side represent targets to be detected.

$l_{m,n}$  via the target location  $l_T$ . For simplicity, we ignore the magnitude term of the Green's function since it can be considered constant for the whole imaging domain.

Without loss of generality we assume there are  $K$  objects in the area of interest, where each object is composed of multiple stationary scattering centers. Moreover, we assume that the array aperture size is small, such that the same scattering centers are observed at all elements of the array. We also discretize the area of interest, using a two-dimensional grid, where index  $i$  denotes each gridpoint, with corresponding location  $l_i$ . Consequently, the received signal can be modeled as the superposition of radar echoes of all  $K$  objects in the area of interest as follows

$$Y(\omega, l_S, l_{m,n}) = \sum_i P(\omega) X(l_i) e^{-j\omega \frac{\|l_S - l_i\| + \|l_{m,n} - l_i\|}{c}}, \quad (3)$$

where  $X(l_i)$  is the reflectivity of a target if it is occupying grid point  $i$  and zero otherwise. This propagation equation can be compactly denoted in a matrix-vector form

$$\mathbf{y}_m = \Phi_m \mathbf{x}_m + \mathbf{e}_m, \quad (4)$$

where  $\mathbf{y}_m$ ,  $\Phi_m$ , and  $\mathbf{x}_m$  represent the samples of the received signal, the forward acquisition process, and the reflectivity corresponding to the  $m$ th array, respectively. Note that the vector  $\mathbf{e}_m$  in the discretized model (4) represents additive acquisition noise.

Assuming that the targets' complex reflectivity coefficients are identical as observed by all the receivers, we can coherently combine the received signals from all the receives as

$$\mathbf{y} = \Phi \mathbf{x} + \mathbf{e}, \quad (5)$$

where  $\mathbf{y} = [\mathbf{y}_1, \dots, \mathbf{y}_M]^T$ ,  $\Phi = [\Phi_1, \dots, \Phi_M]^T$ , and  $\mathbf{x} = \mathbf{x}_1 = \mathbf{x}_2 = \dots = \mathbf{x}_M$ . Again, the vector  $\mathbf{e}$  in (5) represents measurement noise.

The goal of the image formation process is to determine the signal of interest  $\mathbf{x}$  from the array echoes  $\mathbf{y}$  given the acquisition matrix  $\Phi$ . In other words, image formation attempts

to solve a linear inverse problem. If the acquisition matrix  $\Phi$  is invertible, the straightforward choice is to use the inverse or the pseudoinverse of  $\Phi$  to determine  $\mathbf{x}$ , i.e.,

$$\hat{\mathbf{x}} = \Phi^\dagger \mathbf{y}. \quad (6)$$

However, due to the size of  $\Phi$ , the pseudo-inverse  $\Phi^\dagger$  may be difficult to compute and is often not robust to noise. Instead, the more commonly used delay-and-sum beamforming uses the adjoint to estimate  $\mathbf{x}$

$$\hat{\mathbf{x}} = \Phi^H \mathbf{y}. \quad (7)$$

In distributed sensing, sensor arrays are generally non-uniformly distributed in the spatial domain. Therefore, the sidelobes of the beamforming imaging results are generally large (e.g., see [6]), making it difficult to discriminate targets.

### III. COMPRESSIVE SENSING IMAGING

In order to improve the imaging resolution of distributed sensing, we propose two CS-inspired imaging methods. Our first method is based on enforcing image sparsity directly in the spatial domain. However, since spatial-domain sparsity is not strictly true for radar images, we additionally propose a post-processing step to further boost the performance of traditional CS-based radar imaging in the presence of noise. The second method circumvents the post-processing by imposing sparsity in the gradient domain, as measured using the total variation semi-norm. This is a more realistic assumption for radar imaging, where images are often piecewise smooth.

#### A. Image-domain sparsity

The beampattern of a non-uniform array generally exhibits larger sidelobes than a uniform array of the same size. To eliminate the effect of the sidelobes, in the first approach, we interpret the distributed measurements as the downsampled versions of the data from larger distributed uniform arrays, where each large array has about the same aperture size as the total aperture (see yellow dotted lines in Fig. 1). Assuming noiseless acquisition in of (5), we represent the full data on the larger uniform arrays as  $\mathbf{y}_{\text{full}}$ . The vector  $\mathbf{y}_{\text{full}}$  includes the measured data  $\mathbf{y}$  and unmeasured data  $\bar{\mathbf{y}}$  as follows

$$\mathbf{y}_{\text{full}} = \begin{bmatrix} \mathbf{y} \\ \bar{\mathbf{y}} \end{bmatrix} = \begin{bmatrix} \mathbf{E} \\ \bar{\mathbf{E}} \end{bmatrix} \Psi \mathbf{x}. \quad (8)$$

Here,  $\mathbf{E}$  and  $\bar{\mathbf{E}}$  represent complementary down-sampling operators, respectively, and  $\Psi$  denotes the measurement matrix for large uniform aperture arrays.

In traditional CS, the vector  $\mathbf{x}$  is modeled as a sparse signal, which is generally not true in radar imaging. Instead of simply treating  $\mathbf{x}$  as a sparse signal, we propose to decompose  $\mathbf{x}$  into sparse part  $\mathbf{x}_s$  and dense residual  $\mathbf{x}_r$  as

$$\mathbf{x} = \mathbf{x}_s + \mathbf{x}_r. \quad (9)$$

Substituting this expression into (8), the noisy measured data can be expressed as

$$\mathbf{y} = \mathbf{E} \Psi \mathbf{x}_s + \mathbf{E} \Psi \mathbf{x}_r + \mathbf{e}. \quad (10)$$

Treating  $\mathbf{E} \Psi \mathbf{x}_r$  as an additional noise component, the estimate of the sparse component  $\mathbf{x}_s$  is given by

$$\hat{\mathbf{x}}_s = \arg \min_{\mathbf{x}} \|\mathbf{y} - \mathbf{E} \Psi \mathbf{x}\|_{\ell_2}^2 \quad \text{s.t.} \quad \|\mathbf{x}\|_{\ell_0} < N. \quad (11)$$

The above problem can be solved by various compressive sensing solvers. We rely on an iterative algorithm, originally introduced in [7] for SAR applications, which is based on the *Stagewise Orthogonal Matching Pursuit (STOMP)* [8].

Given the sparse estimate  $\hat{\mathbf{x}}_s$ , we estimate its contribution to the measured data as  $\mathbf{E}\Psi\hat{\mathbf{x}}_s$ . We assume the residual data  $\mathbf{y}_r = \mathbf{y} - \mathbf{E}\Psi\hat{\mathbf{x}}_s$  is due to the dense part  $\mathbf{x}_r$ . Thus, we perform a line search to estimate the dense part, such that  $\hat{\mathbf{x}}_s$  and  $\hat{\mathbf{x}}_r$  can be combined properly. In particular,  $\hat{\mathbf{x}}_r = \alpha\Psi^H\mathbf{y}_r$ , where  $\alpha$  is a scalar determined by

$$\alpha = \arg \min_{\alpha} \|\Psi\hat{\mathbf{x}}_r - \mathbf{y}_r\|_{\ell_2}^2 = \arg \min_{\alpha} \|\alpha\Psi\Psi^H\mathbf{y}_r - \mathbf{y}_r\|_{\ell_2}^2. \quad (12)$$

By solving (12), we have

$$\hat{\mathbf{x}}_r = \frac{\mathbf{y}_r^H\mathbf{y}_r}{\mathbf{y}_r^H\Psi\Psi^H\mathbf{y}_r}\Psi^H\mathbf{y}_r. \quad (13)$$

To obtain the final image we combine (11) and (13):

$$\hat{\mathbf{x}} = \hat{\mathbf{x}}_s + \hat{\mathbf{x}}_r. \quad (14)$$

Alternatively, we can estimate the missing data on the large uniform arrays using the sparse estimate  $\hat{\mathbf{x}}_s$  as

$$\bar{\mathbf{y}} = \bar{\mathbf{E}}\Psi\hat{\mathbf{x}}_s. \quad (15)$$

Combining (15) with the measured data, we obtain an estimate of a full data set for the large aperture arrays as

$$\hat{\mathbf{y}}_{\text{full}} = \mathbf{E}^\dagger\mathbf{y} + \bar{\mathbf{E}}^\dagger\bar{\mathbf{E}}\Psi\hat{\mathbf{x}}_s. \quad (16)$$

Note that  $\mathbf{E}$  is a selection operator, and its pseudoinverse  $\mathbf{E}^\dagger$  just fills the missing data with zeros.

Based on the estimated data, we can perform imaging using conventional delay-and-sum beamforming

$$\begin{aligned} \hat{\mathbf{x}} &= \Psi^H\hat{\mathbf{y}}_{\text{full}} = \Psi^H(\mathbf{E}^\dagger\mathbf{y} + \bar{\mathbf{E}}^\dagger\bar{\mathbf{E}}\Psi\hat{\mathbf{x}}_s) \\ &= \Psi^H\Psi\hat{\mathbf{x}}_s + \Psi^H\mathbf{E}^\dagger\mathbf{E}\Psi\hat{\mathbf{x}}_r. \end{aligned} \quad (17)$$

The final images produced by (14) and (17) are not strictly sparse. The output of (14) is generally sharper than that of (17), since the term  $\Psi^H\Psi$  works as a low pass filter, with filtering characteristics related to the large aperture measurement matrix  $\Psi$ . In practice, however, since radar echoes are often noisy, the final imaging result is visually better using (17).

### B. Image gradient-domain sparsity

As an alternative to spatial sparsity, we formulate the gradient-domain algorithm as the following minimization problem

$$\hat{\mathbf{x}}_{\text{TV}} = \arg \min_{\mathbf{x}} \left\{ \frac{1}{2} \|\mathbf{y} - \Phi\mathbf{x}\|_{\ell_2}^2 + \lambda \text{TV}(\mathbf{x}) \right\}, \quad (18)$$

where TV denotes the isotropic total variation regularizer [9]

$$\text{TV}(\mathbf{x}) \triangleq \sum_i \|[\mathbf{D}\mathbf{x}]_i\|_{\ell_2} \quad (19a)$$

$$= \sum_i \sqrt{|[\mathbf{D}_x\mathbf{x}]_i|^2 + |[\mathbf{D}_y\mathbf{x}]_i|^2}. \quad (19b)$$

Here,  $\lambda > 0$  is the regularization parameter and  $[\mathbf{D}\mathbf{x}]_i = ([\mathbf{D}_x\mathbf{x}]_i, [\mathbf{D}_y\mathbf{x}]_i)$  denotes the  $i^{\text{th}}$  component of the image

gradient. Since TV-term in (18) is non-differentiable, we formulate the problem as the following equivalent constrained optimization problem

$$(\hat{\mathbf{x}}, \hat{\mathbf{d}}) = \arg \min_{\mathbf{x}, \mathbf{d}} \left\{ \frac{1}{2} \|\mathbf{y} - \Phi\mathbf{x}\|_{\ell_2}^2 + \lambda \sum_i \|[\mathbf{d}]_i\|_{\ell_2} : \mathbf{d} = \mathbf{D}\mathbf{x} \right\}$$

We solve the constrained optimization problem by designing an *augmented Lagrangian (AL)* scheme [10], specifically, by seeking the critical points of the following cost

$$\begin{aligned} \mathcal{L}(\mathbf{x}, \mathbf{d}, \mathbf{s}) &\triangleq \frac{1}{2} \|\mathbf{y} - \Phi\mathbf{x}\|_{\ell_2}^2 + \lambda \sum_i \|[\mathbf{d}]_i\|_{\ell_2} \\ &\quad + \text{Re}\{\mathbf{s}^H(\mathbf{d} - \mathbf{D}\mathbf{x})\} + \frac{\rho}{2} \|\mathbf{d} - \mathbf{D}\mathbf{x}\|_{\ell_2}^2, \end{aligned} \quad (20)$$

where  $\mathbf{s}$  is the dual variable that imposes the constraint  $\mathbf{d} = \mathbf{D}\mathbf{x}$ , and  $\rho > 0$  is the quadratic penalty parameter. Traditionally, an AL scheme solves the problem (20) by alternating between a joint minimization step and a Lagrangian update step as

$$(\mathbf{x}^{k+1}, \mathbf{d}^{k+1}) \leftarrow \arg \min_{\mathbf{x}, \mathbf{d}} \{\mathcal{L}(\mathbf{x}, \mathbf{d}, \mathbf{s}^k)\} \quad (21a)$$

$$\mathbf{s}^{k+1} \leftarrow \mathbf{s}^k + \rho(\mathbf{d}^{k+1} - \mathbf{D}\mathbf{x}^{k+1}). \quad (21b)$$

However, the joint minimization step (21a) can be computationally intensive. To circumvent this problem, we separate (21a) into a succession of simpler steps. This form of separation is commonly known as the *alternating direction method of multipliers (ADMM)* [11] and can be described as follows

$$\mathbf{d}^{k+1} \leftarrow \arg \min_{\mathbf{d}} \{\mathcal{L}(\mathbf{x}^k, \mathbf{d}, \mathbf{s}^k)\} \quad (22a)$$

$$\mathbf{x}^{k+1} \leftarrow \arg \min_{\mathbf{x}} \{\mathcal{L}(\mathbf{x}, \mathbf{d}^{k+1}, \mathbf{s}^k)\} \quad (22b)$$

$$\mathbf{s}^{k+1} \leftarrow \mathbf{s}^k + \rho(\mathbf{d}^{k+1} - \mathbf{D}\mathbf{x}^{k+1}). \quad (22c)$$

The step in Eq. (22a) admits a closed-form solution

$$[\mathbf{d}^{k+1}]_i \leftarrow \mathcal{T}([\mathbf{D}\mathbf{x}^k - \mathbf{s}^k/\rho]_i; \lambda/\rho),$$

where  $i$  is the pixel number and  $\mathcal{T}$  is the component-wise shrinkage function

$$\mathcal{T}(\mathbf{y}, \tau) \triangleq \arg \min_{\mathbf{x} \in \mathbb{C}^2} \left\{ \frac{1}{2} \|\mathbf{x} - \mathbf{y}\|_{\ell_2}^2 + \tau \|\mathbf{x}\|_{\ell_2} \right\} \quad (23a)$$

$$= \max(\|\mathbf{y}\|_{\ell_2} - \tau, 0) \frac{\mathbf{y}}{\|\mathbf{y}\|_{\ell_2}}. \quad (23b)$$

The step in Eq. (22b) reduces to a linear solution

$$\mathbf{x}^{k+1} = (\Phi^H\Phi + \rho\mathbf{D}^H\mathbf{D})^{-1} (\Phi^H\mathbf{y} + \rho\mathbf{D}^H(\mathbf{d}^{k+1} + \mathbf{s}^k/\rho)).$$

For each iteration  $k = 1, 2, \dots$ , the update rules (22) produce the estimates  $\mathbf{x}^k$  of the true radar image  $\mathbf{x}$ . The final computational time required to obtain the estimate  $\hat{\mathbf{x}}$  depends on the total number of iterations  $k_{\text{max}}$ . In practice, we found that, by using a sufficiently high number of iterations  $k_{\text{max}} = 100$  with an additional stopping criterion based on measuring the relative change of the solution in two successive iterations

$$\frac{\|\mathbf{x}^{k+1} - \mathbf{x}^k\|_{\ell_2}}{\|\mathbf{x}^k\|_{\ell_2}} \leq 10^{-4}, \quad (24)$$

the algorithm achieves excellent results as illustrated in Section IV.

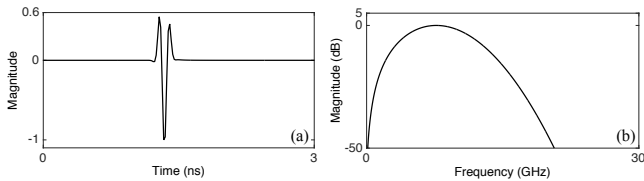


Fig. 2. Pulse emitted by the transmitter in (a) time domain, (b) frequency domain.

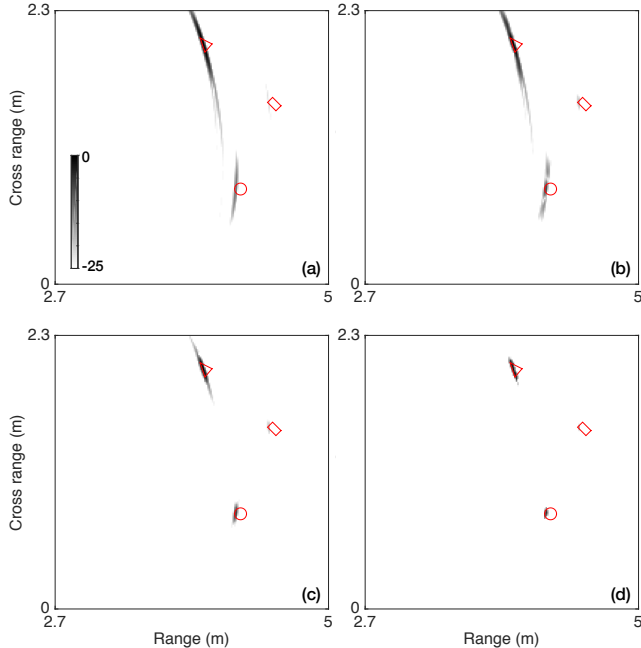


Fig. 3. Imaging results: (a) delay-and-sum beamforming using a single small-aperture array; (b) coherent delay-and-sum beamforming using all four distributed arrays; (c) CS reconstruction with spatial-domain sparsity using all four arrays; (d) CS reconstruction with spatial-gradient-domain sparsity using all four arrays.

#### IV. NUMERICAL EXPERIMENTS

To study the performance of our algorithms, we consider a multi-static experiment depicted in Fig. 1, in which four distributed antenna arrays are used to image three targets in the area of interest. The radar transmitter, denoted by a red  $\times$  in the figure, is located near the four arrays. We use a two-dimensional finite-difference time-domain (FDTD) simulator to emit a differential Gaussian pulse, illustrated in Fig. 2, from the transmitter and record the electric field at all receivers. We simulate noisy measurements by adding noise of SNR = 30 dB to the data before imaging.

The imaging results are plotted in Fig. 3 with 25 dB dynamic range. As evident in Fig. 3(a), the imaging result of a single small aperture array using conventional delay-and-sum beamforming exhibits very coarse azimuth resolution. Figure 3(b) shows that the imaging quality is improved if the beamforming is performed by combining the four distributed arrays coherently, but there still exists strong ambiguity. Instead, our CS-based imaging method with spatial-domain sparsity, shown in Fig. 3(c), suppresses most of the sidelobes and obtains a much tighter focus on the targets, compared to conventional delay-and-sum beamforming. Finally, as we

can see in Fig. 3(d), imposing spatial-gradient-domain sparsity with regularization parameter  $\lambda = 10^{-4}$  further improves the quality of the image by removing isolated noisy pixels and yielding a sharp focus on the targets.

#### V. DISCUSSION

We employ sparsity-driven methods to improve radar imaging using distributed sensor arrays. Our approach exploits the structure of the imaged area, either in the form of spatial sparsity or sparsity in the gradient. Even though our approach is computationally more expensive than conventional beamforming, it also demonstrates significantly improved the imaging quality. Our approach relies on sparse and variational methods, well-established in the context of compressive sensing and ill-posed inverse problems. While our numerical simulations demonstrate the effectiveness in a specific application, our results are further evidence of the benefits of sparsity-driven approaches in radar imaging applications.

One of the drawbacks of our approach, is the assumption of perfect synchronization among sensors and perfect knowledge of the sensor geometry. In practice, synchronization to the desired accuracy and knowledge of the sensor position might not be available. Our goal is to extend our approach to handle imperfect information on timing and location of the sensors. However, we defer that for a future publication.

#### REFERENCES

- [1] E. Candes, J. Romberg, and T. Tao, "Robust uncertainty principles: Exact signal reconstruction from highly incomplete frequency information," *IEEE Transactions on Information Theory*, vol. 52(2), February 2006.
- [2] R. Baraniuk and P. Steeghs, "Compressive radar imaging," in *IEEE Radar Conference*, MA, April 2007.
- [3] M. A. Herman and T. Strohmer, "High-resolution radar via compressed sensing," *IEEE Trans. Signal Process.*, vol. 57, June 2009.
- [4] L. C. Potter, E. Ertin, J. T. Parker, and M. Cetin, "Sparsity and compressed sensing in radar imaging," *Proceedings of the IEEE*, vol. 98, pp. 1006–1020, June 2010.
- [5] P. T. Boufounos, "Depth sensing using active coherent illumination," in *Proc. IEEE Int. Conf. Acoustics, Speech, and Signal Processing (ICASSP)*, Kyoto, Japan, March 25–30 2012.
- [6] L. Li, P.T. Boufounos, D. Liu, H. Mansour, and S. Sahinoglu, "Sparse mimo architectures for through-the-wall imaging," in *IEEE Sensor Array and Multichannel Signal Processing Workshop (SAM)*, June 2014, pp. 513 – 516.
- [7] D. Liu and P. T. Boufounos, "Random steerable arrays for synthetic aperture imaging," in *IEEE International conference on Acoustics Speech and Signal Processing (ICASSP)*, 2013.
- [8] D.L. Donoho, Y. Tsaig, I. Drori, and J.-L. Starck, "Sparse solution of underdetermined systems of linear equations by stagewise orthogonal matching pursuit," *IEEE Trans. Information Theory*, February 2012.
- [9] A. Beck and M. Teboulle, "Fast gradient-based algorithm for constrained total variation image denoising and deblurring problems," *IEEE Trans. Image Process.*, vol. 18, no. 11, pp. 2419–2434, November 2009.
- [10] M. Tao and J. Yang, "Alternating direction algorithms for total variation deconvolution in image reconstruction," *TR0918, Department of Mathematics, Nanjing University*, 2009.
- [11] S. Boyd, N. Parikh, E. Chu, B. Peleato, and J. Eckstein, "Distributed optimization and statistical learning via the alternating direction method of multipliers," *Foundations and Trends in Machine Learning*, vol. 3, no. 1, pp. 1–122, 2011.